PHILOSOPHICAL MAGAZINE, 21 June 2004
VOL. 84, NO. 18, 1889–1905

Taylor & Francis
Taylor & Francis Group

Phase stability and ordering in diluted magnetic III–V semiconductors

V. DRCHAL†, J. KUDRNOVSKÝ†, I. TUREK‡§, F. MÁCA†
and P. WEINBERGER‖¶

† Institute of Physics, Academy of Sciences of the Czech Republic, Na Slovance 2, CZ-182 21 Praha 8, Czech Republic
‡ Institute of Physics of Materials, Academy of Sciences of the Czech Republic, Žižkova 22, CZ-616 62 Brno, Czech Republic
‖ Center for Computational Materials Science, Technical University of Vienna, Getreidemarkt 9/134, A-1060 Vienna, Austria
§ Department of Electronic Structures, Charles University, Ke Karlovu 5, CZ-121 16 Praha 2, Czech Republic

[*Received 14 November 2003 and accepted 17 November 2003*]

ABSTRACT

We study the energetics of diluted ferromagnetic III–V semiconductors on an *ab initio* level using the tight-binding linear muffin-tin orbital–coherent potential approximation method and treating magnetic disorder within the disordered local moment model. Based on calculated total energies, we examine the stability of these alloys with respect to segregation and estimate formation energies of antisite defects and substitutional and interstitial Mn atoms. By using the generalized perturbation method, we calculate the parameters of an effective alloy Ising Hamiltonian including long-range Coulomb interactions. We investigate possible types of ordering, that is correlations of spatial positions of defects using the linearized concentration wave method and Warren–Cowley short-range-order parameters. The theory is illustrated for a $Ga_{1-x}Mn_xAs$ alloy system.

§ 1. INTRODUCTION

Diluted magnetic III–V semiconductors (DMSs) such as $Ga_{1-x}Mn_xAs$ alloys represent a new class of promising materials with potential applications in spin electronics (Ohno 1999). The samples are usually prepared by molecular-beam epitaxy (MBE) on GaAs substrates at temperatures ranging from 200°C to 300°C. Higher temperatures or a Mn content higher than 7 at.% can lead to precipitation of MnAs. According to measurements (Matsukura *et al.* 1998, Ohno *et al.* 1999) of Hall resistivities in strong magnetic fields the conductivity is of p type. Extended X-ray absorption fine-structure studies have shown (Shioda *et al.* 1998) that Mn is substitutionally incorporated into the Ga sublattice and creates a hole in the valence band. Electron spin resonance measurements (Schneider *et al.* 1987) have indicated that substitutional Mn atoms with spin $S = \frac{5}{2}$ are weakly coupled to delocalized holes of opposite projection of spin.

¶Email: pw@cms.tuwien.ac.at.

Philosophical Magazine ISSN 1478–6435 print/ISSN 1478–6443 online
http://www.tandf.co.uk/journals
DOI: 10.1080/14786430310001657364

These materials are highly compensated; that is, the experimentally observed number of holes in the valence band is considerably smaller than the concentration of Mn impurities. This indicates the presence of other lattice defects acting as donors. The most probable candidate for such a compensation are As antisites that would contribute two electrons. Other possibilities are conceivable; in particular, Mn atoms could occupy interstitial positions in the zincblende structure. Such interstitials would act as double donors (Mašek and Máca 2001, Máca and Mašek 2002). Channelling Rutherford back-scattering (Yu *et al.* 2002) and particle-induced X-ray emission experiments have shown that Mn interstitials are highly mobile and their concentration decreases upon annealing. According to a theoretical analysis (Erwin and Petukhov 2002), the Mn atoms are incorporated in interstitial positions in an early stage of the growth process and subsequently after deposition of further Ga and As atoms are incorporated as substitutional impurities.

A sufficiently high Curie temperature is necessary for practical applications. The highest value usually reported for $Ga_{1-x}Mn_xAs$ alloys is 110 K (Matsukura *et al.* 1998, Potashnik *et al.* 2002), while for $Ga_{1-x}Mn_xN$ alloys it is 348 K (Reed *et al.* 2001). Very recently, even higher values for $Ga_{1-x}Mn_xAs$ were achieved by carefully tuning the conditions of the annealing process: Edmonds *et al.* (2002) found 140 K ($x = 0.06$) and Ku *et al.* (2002) reported 150 K. There are, however, indications that this enhancement could be, at least partially, a consequence of surface effects (Ku *et al.* 2002, Sørensen *et al.* 2002).

It is often assumed that the defects are randomly distributed; however, experiments (Potashnik *et al.* 2001) suggested that impurities can diffuse rapidly at 250°C, which is a typical growth and annealing temperature for $Ga_{1-x}Mn_xAs$ samples prepared by MBE. In this case, the spatial distribution of impurities is no longer random, but it becomes (at least partially) correlated (Timm *et al.* 2002). These correlations can substantially modify the transport and magnetic properties of the DMSs.

Here we investigate the phase stability of the DMSs and spatial correlations of impurities in the DMSs from first principles and by employing methods of statistical physics. One has to keep in mind, however, that the samples studied in experiment need not be in thermodynamic equilibrium but rather are in a metastable state corresponding to a local minimum in the thermodynamical potential. Such a state can be relatively stable owing to the energy barriers that lead to extremely slow relaxation. Studies based on equilibrium thermodynamics can nevertheless provide valuable information on certain trends in the structural evolution of DMSs and with respect to their stability.

The paper is organized as follows. In § 2 we briefly describe our approach. Based on *ab initio* electronic structure calculations, we determine the total energies of the disordered alloys as a function of their chemical composition. The results for $Ga_{1-x}Mn_xAs$ alloys are discussed in § 3. The main emphasis is on the determination of formation energies of various impurities (substitutional and interstitial Mn, and As antisites) and on the stability of alloys with respect to segregation. Based on the generalized perturbation method (GPM), we evaluate effective interatomic interactions between impurities including also the long-range Coulomb interactions. We then analyse possible ordering using the linearized version of the concentration wave method and determine the Warren–Cowley short-range-order parameters that yield information about the spatial correlations of the impurities. The conclusions are summarized in § 4.

§ 2. Theory

2.1. *Electronic structure*

The electronic structure is determined using the *ab initio* all-electron scalar–relativistic tight-binding (TB) linear muffin-tin orbital (LMTO) method in the atomic-sphere approximation (ASA) (Turek *et al.* 1997). The underlying lattice, zinc-blende structure, refers to fcc Bravais lattice with a basis which contains a cation site (at $a(0,0,0)$), an anion site (at $a(\frac{1}{4},\frac{1}{4},\frac{1}{4})$), and two interstitial sites occupied by empty spheres (I_1 at $a(\frac{1}{2},\frac{1}{2},\frac{1}{2})$ and I_2 at $a(\frac{3}{4},\frac{3}{4},\frac{3}{4})$) which are necessary for a correct description of open lattices (Glötzel *et al.* 1980, Kudrnovský *et al.* 1989) within the ASA.

The anion sublattice is occupied only by As atoms, while the cation sublattice is occupied by Ga and substitutional Mn atoms, and also by As antisite defects. We also consider the possibility that the interstitial sites I_1 and I_2 can be occupied by Mn atoms. The substitutional disorder on the cation sublattice and on the interstitial sublattice can be described within the coherent potential approximation (CPA) (Kudrnovský *et al.* 1989, Turek *et al.* 1997). We thus neglect local environment effects and lattice relaxations. Note that the CPA also allows us to calculate the properties of a single impurity by setting its concentration equal to zero.

In metallic alloys, where charge transfer is rather weak, it is possible to vary sphere radii so as to achieve zero net charges (Turek *et al.* 1997). In the present case such a procedure would lead to large changes in the radii and, moreover, would be unphysical, because it would not take into account a genuine charge transfer between the cation and anion atoms in DMSs. In addition, it cannot be applied to empty spheres used in the present formalism. We therefore assume equal volumes of spheres such that their sum equals the volume of the system. The non-zero net charges require that in the atomic potentials the Madelung potential is included (for details see appendix A). We made no attempt to include the screening of atomic charges because, in the DMSs, one cannot expect efficient screening owing to a low concentration of free carriers.

In addition to substitutional randomness, some degree of magnetic disorder (Schliemann *et al.* 2001, Korzhavyi *et al.* 2002) is typical for DMSs which we treat in terms of the disordered local moment (DLM) method (Pindor *et al.* 1983, Akai and Dederichs 1993, Turek *et al.* 1997) that can be naturally incorporated in the CPA. The Mn atoms then have collinear, but random spin-up ($Mn^{\uparrow}$) and spin-down ($Mn^{\downarrow}$) orientations, their concentrations being $x^{\uparrow}$ and $x^{\downarrow}$ respectively. The degree of magnetic order can be characterized by the parameter $r=(x^{\uparrow}-x^{\downarrow})/x$, where $x=x^{\uparrow}+x^{\downarrow}$. For example, a GaAs mixed crystal with Mn and As atoms on the Ga sublattice, with respective concentrations x and y, is treated as a multicomponent alloy $(Ga_{1-x-y}Mn^{\uparrow}_{(1+r)x/2}Mn^{\downarrow}_{(1-r)x/2}As_y)As$. In the ferromagnetic (FM) state, $r=1$; that is, all Mn magnetic moments are aligned in the direction of a global magnetization. The paramagnetic (PM) state, $r=0$, corresponds to a complete disorder of spin directions. Besides the FM and PM states (Akai 1998, Schulthess and Butler 2001) a partial ferromagnetic (pFM) state, $0<r<1$, is possible in which spin orientations are partially disordered. A possible magnetic disorder of interstitial Mn atoms can be treated in the same way.

One has to be aware of the fact that treating the $Mn^{\uparrow}$ and $Mn^{\downarrow}$ atoms within the DLM as alloy constituents needs some care as their individual concentrations need not be conserved in a real alloy. Our approach is similar to that of the fixed-spin

method (Moruzzi *et al.* 1986); we first make calculations for fixed concentrations of $Mn^{\uparrow}$ and $Mn^{\downarrow}$ atoms and then search for minimum of the energy.

2.2. *Ising Hamiltonian*

A particular configuration of a homogeneous disordered multicomponent alloy is characterized by occupation indices $\{\eta_{\mathbf{R}}^{Q}\}$, where $\eta_{\mathbf{R}}^{Q}=1$ if the site $\mathbf{R}$ is occupied by an atom of type Q, and $\eta_{\mathbf{R}}^{Q}=0$ otherwise. Configurational averaging of occupation indices $\langle\eta_{\mathbf{R}}^{Q}\rangle = c^{Q}$ yields the concentrations c^{Q}. The energy of such configuration can be expressed in the form of an effective Hamiltonian of Ising type:

$$H = E_0 + \sum_{\mathbf{R}Q} D_{\mathbf{R}}^{Q}\,\eta_{\mathbf{R}}^{Q} + \frac{1}{2}\sum_{\mathbf{R}\mathbf{R}'}\sum_{QQ'} V_{\mathbf{R}\mathbf{R}'}^{QQ'}\,\eta_{\mathbf{R}}^{Q}\,\eta_{\mathbf{R}'}^{Q'} + \cdots, \tag{1}$$

whose parameters are the configurationally independent part of the alloy internal energy E_0, the on-site energies $D_{\mathbf{R}}^{Q}$, the interatomic pair interactions $V_{\mathbf{R}\mathbf{R}'}^{QQ'}$ and, in general, interatomic interactions of higher order. In homogeneous alloys (which is our case if we consider disorder on one sublattice), the first two terms in equation (1) do not depend on the alloy configuration and will therefore be omitted in the following. For simplicity we limit ourselves to pair interactions only, although in principle triplets, quadruplets, etc., can be included.

The pair interactions $V_{\mathbf{R}\mathbf{R}'}^{QQ'}$ in DMSs consist of two contributions:

$$V_{\mathbf{R}\mathbf{R}'}^{QQ'} = v_{\mathbf{R}\mathbf{R}'}^{QQ'} + \phi_{\mathbf{R}\mathbf{R}'}^{QQ'}, \tag{2}$$

where the $v_{\mathbf{R}\mathbf{R}'}^{QQ'}$ result from a mapping of the band part of the total energy on to the Ising Hamiltonian (1) and the $\phi_{\mathbf{R}\mathbf{R}'}^{QQ'}$ refer to the electrostatic interaction energy of a given pair of atoms Q, Q' located at sites $\mathbf{R}, \mathbf{R}'$ (for derivation see appendix A),

$$\phi_{\mathbf{R}\mathbf{R}'}^{QQ'} = \frac{e^2 q_{\mathrm{eff}}^{Q} q_{\mathrm{eff}}^{Q'}}{|\mathbf{R}-\mathbf{R}'|}, \tag{3}$$

where $q_{\mathrm{eff}}^{Q} = q^{Q} - \bar{q}$ is the effective net charge of atomic species Q defined as a difference of the net charge q^{Q} of atomic species Q and the averaged charge $\bar{q}$. The band term contribution is calculated using the GPM (Ducastelle 1991, Drchal *et al.* 1996, Turek *et al.* 1997):

$$v_{\mathbf{R}\mathbf{R}'}^{QQ'} = \frac{1}{\pi}\mathrm{Im}\left(\int_{E_{\min}}^{E_{\mathrm{F}}} \mathrm{d}E\,\mathrm{Tr}\left[t_{\mathbf{R}}^{Q}(z)\bar{g}_{\mathbf{R}\mathbf{R}'}(z)t_{\mathbf{R}'}^{Q'}(z)\bar{g}_{\mathbf{R}'\mathbf{R}}(z)\right]\right), \tag{4}$$

where Tr denotes a trace over angular momentum indices (ℓm) and the spin index σ, $z = E + \mathrm{i}0$, E_{F} is the CPA Fermi energy, $E_{\min}$ is a suitably chosen energy below the valence energy spectrum, $\bar{g}_{\mathbf{R}\mathbf{R}'}(z)$ denotes the block of the averaged auxiliary Green function between sites $\mathbf{R}$ and $\mathbf{R}'$, and $t_{\mathbf{R}}^{Q}(z)$ is the $\mathbf{t}$ matrix for atomic species Q.

It is advantageous to eliminate one of the atomic species, say Ga (further denoted with a superscript 0) using the transformation $\eta_{\mathbf{R}}^{0} = 1 - \sum_{Q}' \eta_{\mathbf{R}}^{Q}$ which converts equation (1) into the form

$$H = E_0' + \tfrac{1}{2}\sum_{\mathbf{R}\mathbf{R}'}\sum_{QQ'}{}' \widetilde{V}_{\mathbf{R}\mathbf{R}'}^{QQ'}\,\eta_{\mathbf{R}}^{Q}\,\eta_{\mathbf{R}'}^{Q'}, \tag{5}$$

where the primed sum denotes summation over $Q \neq 0$, $Q' \neq 0$, and

$$\widetilde{V}_{\mathbf{R}\mathbf{R}'}^{QQ'} = V_{\mathbf{R}\mathbf{R}'}^{QQ'} + V_{\mathbf{R}\mathbf{R}'}^{00} - V_{\mathbf{R}\mathbf{R}'}^{Q0} - V_{\mathbf{R}\mathbf{R}'}^{0Q'}. \tag{6}$$

2.3. *Computational procedure*

We neglect changes in the lattice constant due to the varying composition and assume the lattice constant $a = 5.652$ Å. We use equal radii of the Wigner–Seitz spheres for all atomic species and for the empty spheres ($R_{\mathrm{WS}} = 2.63$ Bohr), which leads to a considerable charge transfer between the alloy constituents (see § 3.1 below), and the Vosko–Wilk–Nusair (1980) parametrization of the exchange–correlation energy.

The energy integration is performed along a contour in the upper half of the complex energy plane, and the **k**-space integration over the irreducible wedge of the Brillouin zone using usually 280 points. We have verified that 1638 points lead to very similar results, the difference in the E_{tot} being less than 2 μRy.

The computation of the lattice Fourier transform of the $v_{\mathbf{RR}'}^{QQ'}$ is trivial, but that of the $\phi_{\mathbf{RR}'}^{QQ'}$, (equation (3)) has to be performed by employing the Ewald summation technique (Born and Huang 1954) which leads to

$$\sum_{\mathbf{R}\neq\mathbf{0}} \frac{\exp(\mathrm{i}\mathbf{k}\cdot\mathbf{R})}{|\mathbf{R}|} = -\frac{1}{\rho\pi^{1/2}} + \frac{4\pi}{\Omega_0}\sum_{\mathbf{K}} \frac{\exp\{-[\rho(\mathbf{k}+\mathbf{K})]^2\}}{|\mathbf{k}+\mathbf{K}|^2} + \sum_{\mathbf{R}\neq\mathbf{0}} \exp(\mathrm{i}\mathbf{k}\cdot\mathbf{R})\frac{\mathrm{erfc}(|\mathbf{R}|/2\rho)}{|\mathbf{R}|}, \tag{7}$$

where Ω_0 is the volume of an elementary cell, **K** denotes lattice vectors of the reciprocal lattice, and the optimal value for ρ is $\rho = \Omega_0^{1/3}/2\pi^{1/2}$.

§ 3. Results and discussion

3.1. *Electronic and magnetic structure*

All calculations of the electronic structure were performed for p-type alloys $Ga_{1-x}Mn_xAs$. First, we considered alloys $(Ga_{1-x-y}Mn_xAs_y)As$ with As antisites, but without interstitial Mn atoms in the concentration range $0 \leqslant y \leqslant x/2$, $0 \leqslant x \leqslant 0.1$, with steps $\Delta x = 0.01$ and $\Delta y = 0.0025$. In order to find the ground state, we varied the order parameter r in steps $\Delta r = 0.05$ for each composition (x, y) and evaluated the total energy. The local moments $m(\mathrm{Mn}^{\uparrow})$ and $m(\mathrm{Mn}^{\downarrow})$ have opposite signs and are nearly of the same value (about $4\,\mu_{\mathrm{B}}$). They depend only weakly on the composition. As a result, the magnetization in the pFM state, $m \approx x^{\uparrow}m(\mathrm{Mn}^{\uparrow}) + x^{\downarrow}m(\mathrm{Mn}^{\downarrow})$, is strongly reduced (Korzhavyi *et al.* 2002) compared with the FM state. The magnetization is zero in the PM regime owing to a complete orientational disorder of local moments.

In the next step we considered alloys of the type $(Ga_{1-x-y-z}Mn_xAs_y)AsMn_z^{(\mathrm{i})}$ containing also interstitial Mn atoms ($Mn^{(\mathrm{i})}$). From the assumption that the alloy is of p type it follows that $2y + 3z \leqslant c(\mathrm{Mn})$. We assumed a fixed total concentration $c(\mathrm{Mn}) = x + z = 0.06$ of Mn atoms and variable concentration y of As antisites in steps $\Delta y = 0.0025$. The interstitial Mn atoms can occupy the tetrahedral positions I_1 or I_2 and also a hexagonal position $a(\frac{5}{8}, \frac{5}{8}, \frac{5}{8})$. The Mn atoms in positions I_1 and I_2 can be described within the TB LMTO–CPA formalism in a straightforward manner, while this is not possible for interstitials in the hexagonal position.

First, we made calculations for Mn atoms at I_1. In searching for the ground state, we varied the order parameters $r = (x^{\uparrow} - x^{\downarrow})/x$, $0 \leqslant r \leqslant 1$, in steps $\Delta r = 0.05$ and $s = (z^{\uparrow} - z^{\downarrow})/z$, $-1 \leqslant s \leqslant 1$ in steps $\Delta s = 0.05$ for each composition (x, y, z) and

Table 1. Valences, averaged numbers N_{el}^{Q} of valence electrons, net charges q^{Q}, effective charges q_{eff}^{Q} and magnetic moments m^{Q} of atoms Q in the $(Ga_{0.935}Mn_{0.04}^{\uparrow}Mn_{0.01}^{\downarrow}As_{0.015})As(E_{0.99}^{(1)}Mn_{0.01}^{\downarrow})E^{(2)}$ alloy.

Site	Atom	Valence	N_{el}^{Q}	q^{Q}	q_{eff}^{Q}	m^{Q} (μ_{B})
Cation	Ga	3	2.346 89	−0.653 11	0.002 14	0.003 55
	$Mn^{\uparrow}$	7	6.349 80	−0.650 20	0.005 05	3.919 14
	$Mn^{\downarrow}$	7	6.354 31	−0.645 69	0.009 57	−3.934 06
	As	5	4.191 35	−0.808 65	−0.153 39	0.008 06
Anion	As	5	4.230 45	−0.769 55	0.000 00	0.000 28
I_1	E	0	0.774 11	0.774 11	0.006 43	0.002 25
	$Mn^{\uparrow}$	7	7.119 37	0.119 37	−0.648 31	3.061 48
	$Mn^{\downarrow}$	7	7.131 28	0.131 28	−0.636 40	−2.962 62
I_2	E	0	0.657 13	0.657 13	0.000 00	0.006 03

evaluated the total energy. We have found that in the ground state (whenever the concentration of interstitial Mn atoms $z > 0$) the moments of interstitial Mn atoms are completely aligned opposite to the moments of the substitutional Mn atoms ($0 < r \leqslant 1$ and $s = -1$).

Similar calculations for Mn atoms at I_2 have shown that in the ground state the moments of interstitial Mn atoms are completely aligned in the direction of the net magnetization of substitutional Mn atoms ($0 < r \leqslant 1$ and $s = +1$). We found that the total energy of the alloy with Mn atoms at I_2 is always higher than the energy of the alloy of the same composition with Mn atoms at I_1. The typical difference was several hundred micro-Rydbergs per unit cell. Our calculations based on the full-potential augmented-plane-wave method lead to similar results for interstitials at I_1 and I_2 and have shown that the interstitial Mn atom in the hexagonal position has energy higher by 38 mRy than that at I_1. We thus pay main attention to the I_1 interstitials.

In table 1 we list the local charges and magnetic moments for one typical composition of the alloy. As we use equal radii of the Wigner–Seitz spheres for all atomic species and for empty spheres, a considerable charge transfer between the alloy constituents is observed. The local moments on substitutional Mn atoms are very similar to those in alloys without interstitials, while the local moments $m(Mn^{(i)}\uparrow)$ and $m(Mn^{(i)}\downarrow)$ on interstitial Mn atoms (about $\pm 3\mu_{\mathrm{B}}$) are approximately by $1\mu_{\mathrm{B}}$ smaller than the moments on substitutional Mn atoms. The electron configuration of a substitutional Mn atom can be roughly expressed as $s^{0.50}p^{0.57}d^{5.28}$, where the exponents denote the number of s, p and d electrons in the atomic sphere. The configuration of an interstitial Mn atom at I_1 is different: $s^{0.52}p^{0.60}d^{6.01}$. At the same alloy composition, the electron configuration of an interstitial Mn atom at I_2 is $s^{0.46}p^{0.50}d^{6.12}$ and its 'up' magnetic moment is surprisingly low, namely $0.245\mu_{\mathrm{B}}$ for $Mn^{\uparrow}$, while for $Mn^{\downarrow}$ we find $-2.963\mu_{\mathrm{B}}$, which is almost identical with the value found for $Mn^{\downarrow}$ at I_1.

3.2. *Energetics of alloys without interstitial Mn atoms*

The calculated total energies (per elementary cell) enable us to investigate impurity formation energies and the stability of $(Ga_{1-x-y}Mn_xAs_y)As$ alloys with respect to segregation into systems with extremal chemical composition.

The formation energy $\varepsilon[A_B]$ of an impurity A_B which substitutes a host atom B in a (generally multicomponent) alloy A_xB_{1-x} is defined as

$$\varepsilon[A_B] = NE[A_{x+\delta x}B_{1-x-\delta x}] + E_{at}[B] - \{NE[A_xB_{1-x}] + E_{at}[A]\}, \quad (8)$$

where N is the number of elementary cells in the alloy, $\delta x = 1/N$, $E_{at}[A]$ is the energy of an isolated atom A and $E[A_xB_{1-x}]$ is the energy of the alloy per one elementary cell. On expanding into linear terms in δx, one finds that (Mašek *et al.* 2002)

$$\varepsilon[A_B] = \frac{\partial E[A_xB_{1-x}]}{\partial x} + E_{at}[B] - E_{at}[A]. \quad (9)$$

We have calculated the total energies for isolated atoms Ga, Mn and As within the local spin-density approximation using the same form of the exchange and correlation energy as for the bulk alloys assuming electron configurations corresponding to the ground state of atoms, namely, $3d^54s^2$ ($^6S_{5/2}$) for Mn, $3d^{10}4s^24p^1$ ($^2P_{1/2}$) for Ga, and $3d^{10}4s^24p^3$ ($^4S_{3/2}$) for As. Figure 1 shows the formation energy of As antisite defect as a function of x(Mn). The formation energy is in all cases a decreasing function of x. It is reduced approximately by 0.01 Ry, if the Mn concentration increases by a few atomic per cent. This means that the number of the antisite defects can be considerably enhanced in the presence of substitutional Mn. This effect may contribute to the self-compensation behaviour of (Ga, Mn)As alloys.

Similarly, the formation energy of the substitutional Mn (figure 2) also decreases with an increasing concentration y of As antisites. The changes in the formation energy $\varepsilon[Mn_{Ga}]$ are again of the order of 0.01 Ry. This means that the presence of As antisites (and probably also of other donors (Mašek *et al.* 2002)) is important for an improved solubility of Mn in III–V materials.

The decreasing character of both $\varepsilon[As_{Ga}]$ and $\varepsilon[Mn_{Ga}]$ indicates a tendency to correlation between these two impurities. The correlation is symmetrical because the slopes of both impurity formation energies are identical as they are equal to

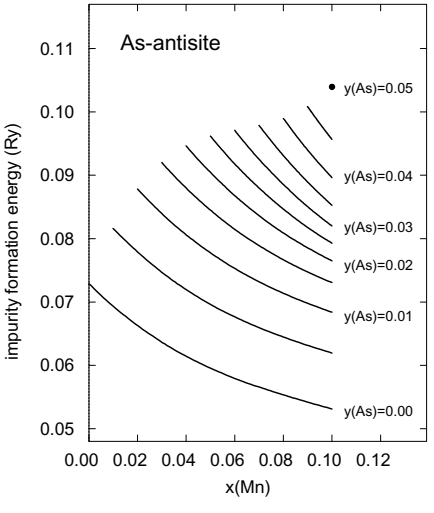

Figure 1. Dependence of the As antisite formation energy $\varepsilon[As_{Ga}]$ on the concentration x of Mn acceptors for various concentrations y of the antisite defects. Note that for y(As)=0.05 there is only a single point.

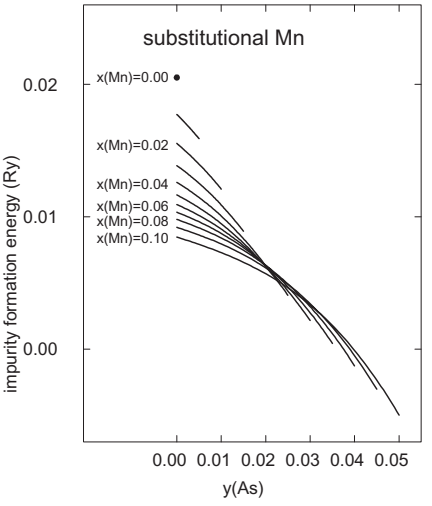

Figure 2. Changes in the formation energy $\varepsilon[\mathrm{Mn_{Ga}}]$ of substitutional Mn in $(\mathrm{Ga}_{1-x-y}\mathrm{Mn}_x\mathrm{As}_y)\mathrm{As}$ alloys due to the As antisite defects. Note that for $x(\mathrm{Mn})=0$ there is only a single point.

the second (mixed) derivative of the total energy with respect to x and y. This quantity is negative in the present case of preferential co-doping.

Let us now consider segregation into an alloy $(\mathrm{Ga}_{1-x}\mathrm{Mn}_x)\mathrm{As}$ without As antisites and an alloy $(\mathrm{Ga}_{1-3x/2}\mathrm{Mn}_x\mathrm{As}_{x/2})\mathrm{As}$ with the highest possible concentration of As antisites which is still not overcompensated:

$$\begin{aligned}\Delta E_1(x,y) = {} & E[(\mathrm{Ga}_{1-x-y}\mathrm{Mn}_x\mathrm{As}_y)\mathrm{As}] \\ & - \frac{x-2y}{x} E[(\mathrm{Ga}_{1-x}\mathrm{Mn}_x)\mathrm{As}] \\ & - \frac{2y}{x} E[(\mathrm{Ga}_{1-3x/2}\mathrm{Mn}_x\mathrm{As}_{x/2})\mathrm{As}]. \end{aligned} \tag{10}$$

The results are shown in figure 3 and clearly indicate the stabilizing effect of the As antisites. Similarly we can consider segregation into an alloy with the highest possible concentration of As antisites which is still not overcompensated $(\mathrm{Ga}_{1-3x/2}\mathrm{Mn}_x\mathrm{As}_{x/2})\mathrm{As}$ and an alloy with the same concentration of As antisites $(\mathrm{Ga}_{1-x_0-y}\mathrm{Mn}_{x_0}\mathrm{As}_y)\mathrm{As}$, where $x_0 = 0.1$, that is, the highest concentration for which we have data available;

$$\begin{aligned}\Delta E_2(x,y) = {} & E[(\mathrm{Ga}_{1-x-y}\mathrm{Mn}_x\mathrm{As}_y)\mathrm{As}] \\ & - \frac{x_0-x}{x_0-2y} E[(\mathrm{Ga}_{1-3y}\mathrm{Mn}_{2y}\mathrm{As}_y)\mathrm{As}] \\ & - \frac{x-2y}{x_0-2y} E[(\mathrm{Ga}_{1-x_0-y}\mathrm{Mn}_{x_0}\mathrm{As}_y)\mathrm{As}]. \end{aligned} \tag{11}$$

The results, shown in figure 4, indicate that the energy cost of doping GaAs by Mn can be lowered by simultaneous addition of As atoms at antisite positions.

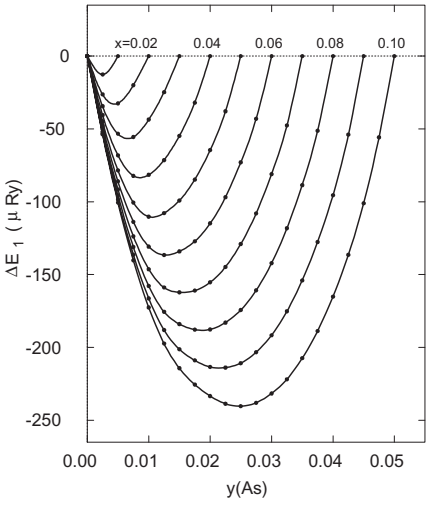

Figure 3. The energy difference $\Delta E_1(x, y)$ for $(Ga_{1-x-y}Mn_xAs_y)As$ alloys (see equation (10)).

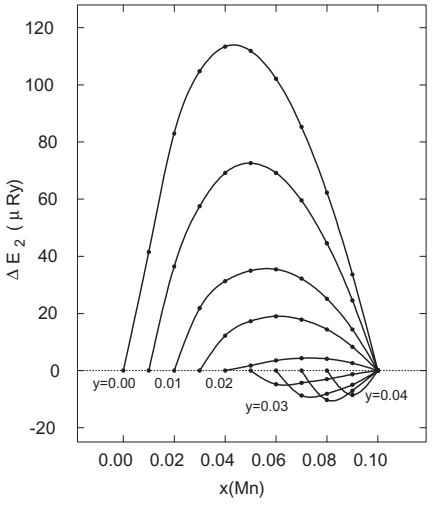

Figure 4. The energy difference $\Delta E_2(x, y)$ for $(Ga_{1-x-y}Mn_xAs_y)As$ alloys (see equation (11)).

These results can also be visualized in a somewhat different form if we consider the segregation into three different compounds, namely GaAs and two alloys $(Ga_{1-x_0}Mn_{x_0})As$ and $(Ga_{1-3x_0/2}Mn_{x_0}As_{x_0/2})As$, where $x_0 = 0.1$ as before. Then

$$\begin{aligned}\Delta E_3(x, y) = {} & E[(Ga_{1-x-y}Mn_xAs_y)As] \\ & - \frac{x_0 - x}{x_0} E[GaAs] \\ & - \frac{x - 2y}{x_0} E[(Ga_{1-x_0}Mn_{x_0})As] \\ & - \frac{2y}{x_0} E[(Ga_{1-3x_0/2}Mn_{x_0}As_{x_0/2})As]. \end{aligned} \tag{12}$$

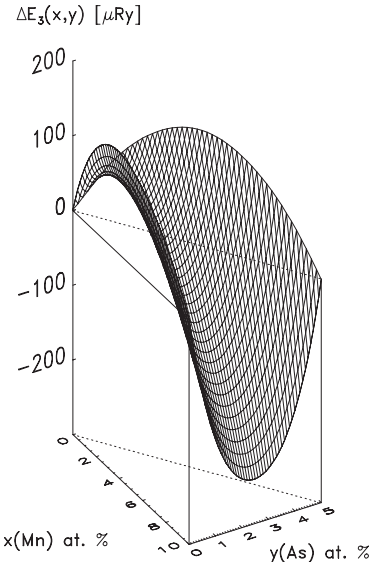

Figure 5. The energy difference $\Delta E_3(x, y)$ for $(Ga_{1-x-y}Mn_xAs_y)As$ alloys (see equation (12)).

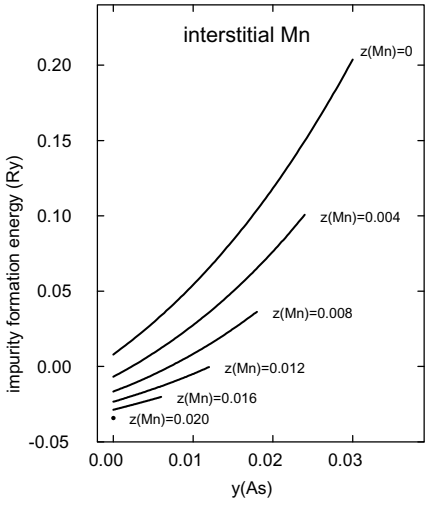

Figure 6. The dependence of the formation energy $\varepsilon[Mn^{(i)}]$ of interstitial Mn in $(Ga_{1-x-y}Mn_xAs_y)AsMn_z^{(i)}$ alloys with $x + z = 0.06$ on the concentration y of the As antisite defects for various concentrations z of interstitial Mn. Note that for z(Mn)=0.02 there is only a single point.

The corresponding results are shown in figure 5. Besides an energy lowering by As antisites, the regimes of instability are visible, particularly close to the lines $y = 0$ and $y = x/2$.

3.3. *Energetics of alloys with interstitial Mn atoms*

The formation energies for interstitial Mn impurities and for As antisites in the presence of interstitials are shown in figures 6 and 7 respectively for constant $c(\mathrm{Mn}) = x + z = 0.06$. The situation is opposite to that found for substitutional

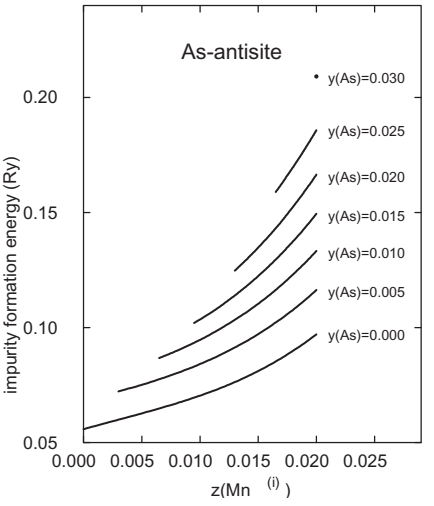

Figure 7. The dependence of the formation energy ε[As] of As antisites in $(Ga_{1-x-y}Mn_x As_y)AsMn_z^{(i)}$ alloys with $x + z = 0.06$ on the concentration z of interstitial Mn for various concentrations of the As antisite defects. Note that for y(As)=0.03 there is only a single point.

Mn because the increasing concentration of one of the species leads to an increase in the impurity formation energy of the other. Also the second mixed derivative of the total energy with respect to y and z is positive. These facts are in agreement with the growth mechanism of $(Ga_{1-x-y}Mn_xAs_y)As$ alloys as discussed by Erwin and Petukhov (2002); the Mn atoms are first incorporated into interstitial positions under a low concentration of As antisites and later, during growth or annealing, as substitutional impurities. In particular, the conversion of the interstitial Mn into a substitutional form is facilitated during the growth process if a sufficient number of As atoms is available, which enters antisite positions.

We note that the impurity formation energy for Mn atom in the interstitial position I_2 is typically higher than that at I_1 by 20–30 mRy.

3.4. *Ordering tendencies*

Our results showed that the effective interatomic pair interactions $V_{\mathbf{RR}'}^{QQ'}$ decrease rather slowly with increasing interatomic distance $|\mathbf{R} - \mathbf{R}'|$ and have to be calculated over many coordination spheres (here we include spheres up to the twenty-ninth neighbour). Moreover, their Coulombic part, even though weak, is long ranged. In order to analyse possible ordering patterns, we employed the linearized concentration-wave method. For temperatures above the ordering temperature T_{ord} we also calculated Warren–Cowley short-range-order parameters. The generalizations to multicomponent alloys needed in our case are described in the appendices B and C. One has to keep in mind that, in these methods, only the configurational part of the entropy is taken into account, which usually leads to an overestimation of ordering temperatures.

As a case study, we made calculations for an alloy of a typical composition $(Ga_{0.93}Mn_{0.03}^{\uparrow}Mn_{0.03}^{\downarrow}As_{0.01})As$ in a non-magnetic state and found an ordering temperature $T_{\mathrm{ord}} = 1067\,\mathrm{K}$. The ordering vector is $\mathbf{k}_0 = (0, 0, 0)$, that is, it corresponds to segregation. The eigenvector $\mathbf{Y}(\mathbf{k}_0)$ yields the following amplitudes: $Y(\mathrm{Ga}) = 0.0$,

Table 2. Warren–Cowley short-range-order parameters for impurities in ($Ga_{0.93}Mn^{\uparrow}_{0.03}Mn^{\downarrow}_{0.03}As_{0.01}$) As alloy at $T = 1100\,K$. Note that owing to a particular composition there exists a symmetry between $Mn^{\uparrow}$ and $Mn^{\downarrow}$ atoms; therefore only the independent parameters are tabulated.

Neighbour	$Mn^{\uparrow}$–$Mn^{\uparrow}$	$Mn^{\uparrow}$–$Mn^{\downarrow}$	As–As	$Mn^{\uparrow}$–As
$(0\,\frac{1}{2}\,\frac{1}{2})$	−2.216	−0.700	0.994	−0.607
(0 0 1)	−0.903	−0.097	−0.262	−0.170
$(\frac{1}{2}\,\frac{1}{2}\,1)$	−0.854	0.034	−0.135	−0.026
(0 1 1)	−0.789	0.065	0.238	−0.189
$(0\,\frac{1}{2}\,\frac{3}{2})$	−0.415	0.069	0.061	−0.056
(1 1 1)	−0.447	0.159	0.085	0.007

$Y(Mn^{\uparrow}) = 0.7071$, $Y(Mn^{\downarrow}) = -0.7071$ and $Y(As) = 0.0$. This type of segregation corresponds to a phase transition to a FM state and is not connected with ordering of Ga atoms and As antisites. Note that T_{ord} is much higher than the Curie temperature T_C of DMSs and that the method of concentration waves leads to a first-order phase transition, while a second-order transition is expected. This is clearly connected with the oversimplified form of entropy, discussed above, in which the terms coresponding to rotations of the magnetic moments are missing.

The results for the Warren–Cowley parameters, summarized in table 2, show a strong tendency to an aggregation of Mn atoms with the same orientation of spin. This finding is in line with the results of van Schilfgaarde and Mryasov (2001) who found a similar tendency. Close pairs of Mn atoms with opposite moments become possible, while the probability to find close pairs of As antisites is very low. A moderate aggregation of Mn atoms and As antisites is also possible.

In the next step we considered a FM alloy ($Ga_{0.93}Mn^{\uparrow}_{0.06}As_{0.01}$)As resulting from the original composition ($Ga_{0.93}Mn^{\uparrow}_{0.03}Mn^{\downarrow}_{0.03}As_{0.01}$)As after transition to a FM state. We find the ordering temperature $T_{ord} = 775\,K$ and the ordering vector $\mathbf{k}_0 = 0.274(1,1,1)/a$. A closer examination shows that the largest eigenvalues of the matrix $\mathbf{\Theta}(\mathbf{k})$ have very similar values (within 1 K) for $\mathbf{k}$ vectors confined within 1% to a surface of a sphere of radius $0.479/a$, which in turn corresponds to a domain of a characteristic radius 37 Å in real space. The eigenvector $\mathbf{Y}(\mathbf{k}_0)$ gives the following amplitudes: $Y(Ga) = 0.726$, $Y(Mn^{\uparrow}) = -0.686$, and $Y(As) = -0.040$. Consequently, domains of two types are formed: in the first type the concentration of impurities Mn and As is increased, while in the second type the impurity concentrations are diminished.

Calculations made for other alloy compositions have shown that the ordering temperature T_{ord} is rather insensitive to the concentration of impurities, while the size of the ordering vector $\mathbf{k}_0 = k_0(1,1,1)/3^{1/2}$ can vary in a broad range.

If only pair interactions $v^{QQ'}_{\mathbf{RR}'}$ are considered, T_{ord} is changed only a little, but $\mathbf{k}_0 = (\pi/a)(0,0,0)$, which corresponds to segregation into a pure GaAs and the rest with a high impurity concentration. Quite obviously, the Coulomb interactions, even though they are weak owing to the small effective net charges, play an important role because they can change qualitatively the ordering behavior of the system. On the other hand, the Warren–Cowley parameters calculated without electrostatic interactions are very similar to those when both types of interaction are included. This result could be expected because weak long-range forces cannot change the short-range order considerably.

§ 4. Conclusions

We have studied the phase stability and the possible ordering in DMSs on an *ab initio* level. The main conclusions of our study can be summarized as follows.

(i) The alloys are thermodynamically unstable with respect to segregation into related compounds or alloys with extremal chemical composition.
(ii) As antisites have a stabilizing effect and make the incorporation of substitutional Mn atoms energetically favourable. On the other hand, incorporation of Mn atoms into interstitial positions is energetically favourable only at low concentration of As antisites.
(iii) Formation of domains of two types, namely with an enhanced and with a lowered concentration of impurities (substitutional Mn atoms and As antisites), can be expected at a critical temperature which is lower than the Curie temperature. The characteric size of the domains depends on chemical composition and might be of order of several tens of ångströms.
(iv) We have found a strong tendency to aggregation of substitutional Mn atoms with the same direction of magnetic moment.
(v) Our results also show that formation of close pairs of As antisites is highly unlikely.

Acknowledgements

Financial support for this work was provided by the Grant Agency of the Academy of Sciences of the Czech Republic (project A1010203), the Ministry of Education, Youth, and Sports of the Czech Republic (COST P5.30 and MSM113200002), the Center for Computational Materials Science in Vienna (GZ 45.504), and the RT Network Computational Magnetoelectronics of the European Commission (contract HPRN-CT-2000-0143). The authors thank Dr J. Mašek for useful discussions.

APPENDIX A

§ A 1. Electrostatic interactions

In this appendix we derive the electrostatic part of the pair interatomic interactions (equation (3)). We assume the ASA and the CPA for the description of randomness and limit ourselves to monopole–monopole interactions only. The parameters of the Ising Hamiltonian (1) are found by expanding the total energy of one configuration of the alloy in terms of occupation indices $\eta_{\mathbf{R}}^{Q}$.

The total energy $E_{\mathrm{tot}} = T + U_{\mathrm{en}} + U_{\mathrm{ee}} + U_{\mathrm{nn}} + E_{\mathrm{xc}}$ of a system of electrons and fixed nuclei within the local spin-density approximation is a sum of the kinetic energy T, the exchange–correlation energy E_{xc} and electrostatic interaction energies between electrons (U_{ee}), between nuclei (U_{nn}) and between electrons and nuclei (U_{en}). The kinetic energy T is usually expressed in terms of the sum $E^{(1)}$ of one-particle energies of the occupied Kohn–Sham states minus the electrostatic energy of electrons in the effective one-electron potential, namely as

$$T = E^{(1)} - \sum_{\mathbf{R}\sigma} \int_{(\mathbf{R})} \rho_{\mathbf{R}\sigma}(r) V_{\mathbf{R}\sigma}(r)\, \mathrm{d}^3\mathbf{r}, \tag{A 1}$$

where (**R**) denotes an integration over the atomic sphere centred at **R**.

The component-dependent ASA potentials that enter the Kohn–Sham equations are

$$V^Q_{\mathbf{R}\sigma}(r) = -\frac{e^2 Z^Q_{\mathbf{R}}}{r} + \int_{(\mathbf{R})} \frac{e^2 \rho^Q_{\mathbf{R}}(r')}{|\mathbf{r}-\mathbf{r}'|}\, \mathrm{d}^3\mathbf{r}' + V^Q_{\mathrm{xc},\mathbf{R}\sigma}(r) + V_{\mathrm{M},\mathbf{R}}, \tag{A 2}$$

where the first term represents the Coulomb potential of nucleus Q at position $\mathbf{R}$, the second term is the electrostatic potential of the charge density $\rho^Q_{\mathbf{R}}(r)$, the third term is the exchange–correlation potential and the last term $V_{\mathrm{M},\mathbf{R}}$ is the Madelung potential which depends on the averaged net charges on all other lattice sites:

$$V_{\mathrm{M},\mathbf{R}} = {\sum_{\mathbf{R}'}}' \frac{e^2 \bar{q}_{\mathbf{R}'}}{|\mathbf{R}-\mathbf{R}'|}, \tag{A 3}$$

where

$$\bar{q}_{\mathbf{R}} = \sum_Q c^Q_{\mathbf{R}}\, q^Q_{\mathbf{R}}, \quad q^Q_{\mathbf{R}} = Q^Q_{\mathbf{R}} - Z^Q_{\mathbf{R}}. \tag{A 4}$$

Here e is the elementary charge, $q^Q_{\mathbf{R}}$ is the net charge and $Q^Q_{\mathbf{R}}$ is the number of electrons within the atomic sphere at site $\mathbf{R}$ occupied by an atom Q. The correlations between the occupation of a particular site $\mathbf{R}$ and the charge densities within the other atomic spheres are neglected. This leads to a component-independent Madelung contribution to $V^Q_{\mathbf{R}\sigma}(r)$ in equation (A 2). In bulk systems (such as DMSs) consisting of several sublattices, the averaged charge transfer with respect to different sublattices is in general non-zero and leads to non-vanishing Madelung terms.

The exchange–correlation energy, approximated by

$$E_{\mathrm{xc}} = \sum_{\mathbf{R}} \int_{(\mathbf{R})} \rho_{\mathbf{R}}(r) \epsilon_{\mathrm{xc}}(\rho_{\mathbf{R}\uparrow}(r), \rho_{\mathbf{R}\downarrow}(r))\, \mathrm{d}^3\mathbf{r}, \tag{A 5}$$

is a sum of single-site terms; so it does not contribute to interatomic interactions. The only contributions to interatomic interactions arise from $E^{(1)}$ (these are calculated within the GPM) and from the interatomic part of the electrostatic interaction energy which obviously is given by

$$\{U_{\mathrm{en}} + U_{\mathrm{ee}} + U_{\mathrm{nn}}\}_{\mathrm{interatomic}} = \tfrac{1}{2} {\sum_{\mathbf{R}\mathbf{R}'}}' \sum_{QQ'} q^Q_{\mathbf{R}}\, \eta^Q_{\mathbf{R}}\, \frac{e^2}{|\mathbf{R}-\mathbf{R}'|}\, q^{Q'}_{\mathbf{R}'}\, \eta^{Q'}_{\mathbf{R}'}, \tag{A 6}$$

where the primed sum implies exclusion of terms with $\mathbf{R} = \mathbf{R}'$. It should be noted that equation (A 6) is a direct consequence of the ASA.

Equation (A 6) can be simplified if $q^Q_{\mathbf{R}}$ is expressed in terms of effective net charges defined as $q^{Q,\mathrm{eff}}_{\mathbf{R}} = q^Q_{\mathbf{R}} - \bar{q}_{\mathbf{R}}$, because $\bar{q}_{\mathbf{R}}$ does not depend on the occupation of the site $\mathbf{R}$. Terms containing $\bar{q}_{\mathbf{R}}$ contribute to the configuration-independent part of the alloy energy E_0 and to on-site energies $D^Q_{\mathbf{R}}$, but not to the pair interactions. In the case of a homogeneous system, equation (A 6) can be further simplified as $q^Q_{\mathbf{R}} = q^Q$ and $\bar{q}_{\mathbf{R}} = \bar{q}$ for all $\mathbf{R}$. Consequently, $q^{Q,\mathrm{eff}}_{\mathbf{R}} = q^{Q,\mathrm{eff}} = q^Q - \bar{q}$. This completes our proof of equation (3).

APPENDIX B

§ B 1. Method of linearized concentration waves

The ordering temperature T_{ord} and the type of ordered structure that appears below T_{ord} can be studied in terms of the concentration-wave method (Khachaturyan 1983, Ducastelle 1991). Here we employ its linearized version (Bose *et al.* 1997) extended to a multicomponent alloy since we consider possible ordering of four atomic species (Ga, $Mn^{\uparrow}$, $Mn^{\downarrow}$ and As) on the cation sublattice. In a mean-field approximation (i.e. assuming a Bragg–Williams form of the entropy (Huang 1963) the free energy is expressed in terms of local concentrations $c_{\mathbf{R}}^{Q}$:

$$F = \tfrac{1}{2}\sum_{\mathbf{R}\mathbf{R}'}\sum_{QQ'} V_{\mathbf{R}\mathbf{R}'}^{QQ'} c_{\mathbf{R}}^{Q} c_{\mathbf{R}'}^{Q'} + k_{\mathrm{B}}T \sum_{\mathbf{R}}\sum_{Q} c_{\mathbf{R}}^{Q} \ln (c_{\mathbf{R}}^{Q}), \tag{B 1}$$

where k_{B} is the Boltzmann constant and T is the temperature. Note that in equation (B 1) the configurationally independent terms are omitted, because they lead to an unimportant constant (Bose *et al.* 1997). Starting from the disordered state, the free energy can be expanded up to quadratic terms in concentration fluctuations $\delta c_{\mathbf{R}}^{Q} = c_{\mathbf{R}}^{Q} - c^{Q}$:

$$F = F_0 + \tfrac{1}{2}\sum_{\mathbf{R}\mathbf{R}'}\sum_{QQ'}\left[V_{\mathbf{R}\mathbf{R}'}^{QQ'} + \frac{k_{\mathrm{B}}T}{c^{Q}}\delta_{\mathbf{R}\mathbf{R}'}\delta_{QQ'}\right]\delta c_{\mathbf{R}}^{Q}\,\delta c_{\mathbf{R}'}^{Q'} \tag{B 2}$$

with terms linear in $\delta c_{\mathbf{R}}^{Q}$ vanishing because $\sum_{\mathbf{R}}\delta c_{\mathbf{R}}^{Q} = 0$ for all Q, and $\sum_{\mathbf{R}'Q'} V_{\mathbf{R}\mathbf{R}'}^{QQ'} c^{Q'}$ is a constant for all $\mathbf{R}$ and Q (for details see Bose *et al.* (1997)). Here F_0 is the free energy in the absence of concentration waves ($c_{\mathbf{R}}^{Q} = c^{Q}$ for all $\mathbf{R}$). Equation (B 2) can be rewritten in terms of a lattice Fourier transform as

$$F = F_0 + \tfrac{1}{2}\sum_{\mathbf{k}}^{\mathrm{BZ}}\sum_{QQ'}\left(V^{QQ'}(\mathbf{k}) + \frac{k_{\mathrm{B}}T}{c^{Q}}\delta_{QQ'}\right)[\delta c^{Q}(\mathbf{k})]^{*}\,\delta c^{Q'}(\mathbf{k}), \tag{B 3}$$

or, in matrix notation, as

$$\Delta F = F - F_0 = \tfrac{1}{2}\sum_{\mathbf{k}}^{\mathrm{BZ}} \mathbf{Y}^{\dagger}(\mathbf{k}) \cdot \left[V(\mathbf{k}) + k_{\mathrm{B}}T\mathbf{C}^{-1}\right]\mathbf{Y}(\mathbf{k})|\epsilon(\mathbf{k})|^2, \tag{B 4}$$

where $[V(\mathbf{k})]_{QQ'} = V^{QQ'}(\mathbf{k})$, and the matrix $\mathbf{C}$ is defined as $[C]_{QQ'} = c^{Q}\delta_{QQ'}$. In equation (B 4) the concentration fluctuations $\delta c^{Q}(\mathbf{k})$ are expressed in terms of a vector $\mathbf{Y}(\mathbf{k})$ and the order parameter $\epsilon(\mathbf{k})$ as $\delta c^{Q}(\mathbf{k}) = Y^{Q}(\mathbf{k})\epsilon(\mathbf{k})$. At sufficiently high temperatures, ΔF is positive definite, because the Hermitian matrix $\mathbf{V}(\mathbf{k}) + k_{\mathrm{B}}T\mathbf{C}^{-1}$ has only positive eigenvalues and thus the high-temperature state is completely disordered ($\epsilon(\mathbf{k}) = 0$ for all $\mathbf{k}$). With decreasing temperature it can become indefinite at T_{ord} because of a vanishing eigenvalue for a critical vector $\mathbf{k}_0$ which determines the period of the concentration wave. The components $Y^{Q}(\mathbf{k})$ of the critical eigenvector determine the amplitude of the concentration wave for each alloy component Q. For each $\mathbf{k}$, the minimization of ΔF, and thus the eigenvalue problem, is subject to the subsidiary condition $\sum_{Q} Y^{Q}(\mathbf{k}) = 0$ which follows from $\sum_{Q}\delta c_{\mathbf{R}}^{Q} = 0$, valid for each $\mathbf{R}$. The ordering temperature is then computed as the largest eigenvalue of the matrix $\mathbf{\Theta}(\mathbf{k}) = -k_{\mathrm{B}}^{-1}\mathbf{C}^{1/2}V(\mathbf{k})\mathbf{C}^{1/2}$.

APPENDIX C

§ C 1. Short-range-order parameters

The Warren–Cowley short-range-order parameters (Ducastelle 1991)

$$\alpha^{QQ'}_{\mathbf{R}\mathbf{R}'} = -\frac{\langle \eta^{Q}_{\mathbf{R}} \eta^{Q'}_{\mathbf{R}'} \rangle - \langle \eta^{Q}_{\mathbf{R}} \rangle \langle \eta^{Q'}_{\mathbf{R}'} \rangle}{\langle \eta^{Q}_{\mathbf{R}} \rangle \langle \eta^{Q'}_{\mathbf{R}'} \rangle} = 1 - \frac{\langle \eta^{Q}_{\mathbf{R}} \eta^{Q'}_{\mathbf{R}'} \rangle}{c^{Q} c^{Q'}} \tag{C 1}$$

provide detailed information on mutual correlations of impurities; they can also be used directly in calculations of transport and magnetic properties. The matrix of the Warren–Cowley parameters can be calculated approximately by means of the Krivoglaz–Clapp–Moss formula in reciprocal space,

$$\alpha(\mathbf{k}) = -\mathbf{D}[\mathbf{M} + \beta \widetilde{V}(\mathbf{k})]^{-1} \mathbf{D}^{\mathrm{T}}, \tag{C 2}$$

where $\beta = (k_{\mathrm{B}} T)^{-1}$, and the matrix $\mathbf{M}$ is defined as

$$[\mathbf{M}]_{QQ'} = \frac{1}{c^{0}} + \delta_{Q,Q'} \frac{1}{c^{Q}}. \tag{C 3}$$

The matrix $\mathbf{D}$ is introduced to ensure a correct normalization of α for $\mathbf{R} = \mathbf{R}'$ which follows from the definition (C 1). Note that, in contrast with Taggart (1979), we use a symmetric normalization. An inverse lattice Fourier transform yields the Warren–Cowley parameters in real space:

$$\alpha^{QQ'}_{\mathbf{R}\mathbf{R}'} = \frac{1}{\boldsymbol{\Omega}_{\mathrm{BZ}}} \int_{(\mathrm{BZ})} \mathrm{d}^{3}\mathbf{k} \, [\alpha(\mathbf{k})]_{QQ'} \exp[-\mathrm{i}\mathbf{k} \cdot (\mathbf{R} - \mathbf{R}')]. \tag{C 4}$$

References

Akai, H., 1998, *Phys. Rev. Lett.*, **81**, 3002.

Akai, H., and Dederichs, P. H., 1993, *Phys. Rev.*, **47**, 8739.

Born, M., and Huang, K., 1954, *Dynamical Theory of Crystal Lattices* (Oxford: Clarendon).

Bose, S. K., Drchal, V., Kudrnovský, J., Jepsen, O., and Andersen, O. K., 1997, *Phys. Rev.*, **55**, 8184.

Drchal, V., Kudrnovský, J., Pasturel, A., Turek, I., and Weinberger, P., 1996, *Phys. Rev.*, **54**, 8202.

Ducastelle, F., 1991, *Order and Phase Stability in Alloys* (Amsterdam: North-Holland).

Edmonds, K. W., Wang, K. Y., Campion, R. P., Neumann, A. C., Farley, N. R. S., Gallagher, B. L., and Foxton, C. T., 2002, arXiv:cond-mat/0209554.

Erwin, S. C., and Petukhov, A. G., 2002, *Phys. Rev. Lett.*, **89**, 227 201.

Glötzel, D., Segal, B., and Andersen, O. K., 1980, *Solid St. Commun.*, **36**, 403.

Huang, K., 1963, *Statistical Mechanics* (New York: Wiley) .

Khachaturyan, A. G., 1983, *Theory of Structural Transformations in Solids* (New York: Wiley).

Korzhavyi, P. A., Abrikosov, I. A., Smirnova, E. A., Bergqvist, L., Mohn, P., Mathieu, R., Svedlindh, P., Sadowski, J., Isaev, E. I., Vekilov, Yu. Kh., and Eriksson, O., 2002, *Phys. Rev. Lett.*, **88**, 187 202.

Ku, K. C., Potashnik, S. J., Wang, R. F., Seong, M. J., Johnston-Halperin, E., Meyers, R. C., Chun, S. H., Mascarenhas, A., Gossard, A. C., Awschalom, D. D., Schiffer, P., and Samarth, N., 2002, arXiv:cond-mat/0210426.

Kudrnovský, J., Drchal, V., Šob, M., Christensen, N. E., and Andersen, O. K., 1989, *Phys. Rev.* B, **40**, 10 029.

Máca, F., and Mašek, J., 2002, *Phys. Rev.* B, **65**, 235 209.

Matsukura, F., Ohno, H., Shen, A., and Sugawara, Y., 1998, *Phys. Rev.* B, **57**, R2037.

Mašek, J., and Máca, F., 2001, *Acta Phys. Polon.* A, **100**, 319.
Mašek, J., Turek, I., Drchal, V., Kudrnovský, J., and Máca, F., 2002, *Acta Phys. Polon.* A, **102**, 673.
Moruzzi, V. L., Marcus, P. M., Schwartz, K., and Mohn, P., 1986, *Phys. Rev. B*, **34**, 1784.
Ohno, H., 1999, *J. Magn. magn. Mater.*, **200**, 110.
Ohno, H., Matsukura, F., Omiya, T., and Akiba, N., 1999, *J. appl. Phys.*, **85**, 4277.
Pindor, A. J., Staunton, J., Stocks, G. M., and Winter, H., 1983, *J. Phys.* F, **13**, 979.
Potashnik, S. J., Ku, C. K., Chun, S. H., Berry, J. J., Samarth, N., and Schiffer, P., 2001, *Appl. Phys. Lett.*, **79**, 1495.
Potashnik, S. J., Ku, C. K., Mahendiran, R., Chun, S. H., Wang, R. F., Samarth, N., and Schiffer, P., 2002, *Phys. Rev.* B, **66**, 012 408.
Reed, M. L., Ritums, M. K., Stadelmaier, H. H., Reed, M. J., Parker, C. A., Bedair, S. M., and El-Masry, N. A., 2001, *Mater. Lett.*, **51**, 500.
van Schilfgaarde, M., and Mryasov, O. N., 2001, *Phys. Rev.* B, **63**, 233 205.
Schliemann, J., König, J., and MacDonald, A. H., 2001, *Phys. Rev.* B, **64**, 165 201.
Schneider, J., Kaufmann, U., Wilkening, W., Baeumler, M., and Köhl, F., 1987, *Phys. Rev. Lett.*, **59**, 240.
Schulthess, T. C., and Butler, W. H., 2001, *J. appl. Phys.*, **89**, 7021.
Shioda, R., Ando, K., Hayashi, T., and Tanaka, M., 1998, *Phys. Rev.* B, **58**, 1100.
Sørensen, B. S., Sadowski, J., Andresen, S. E., and Lindelof, P. E., 2002, arXiv:cond-mat/0210480.
Taggart, G. B., 1979, *Phys. Rev.* B, **19**, 3230.
Timm, C., Schäfer, F., and von Oppen, F., 2002, arXiv:cond-mat/0201411.
Turek, I., Drchal, V., Kudrnovský, J., Šob, M., and Weinberger, P., 1997, *Electronic Structure of Disordered Alloys, Surfaces, and Interfaces* (Boston, Massachusetts: Kluwer.
Vosko, S. H., Wilk, L., and Nusair, M., 1980, *Can. J. Phys.*, **58**, 1200.
Yu, K. M., Walukiewicz, W., Wojtowicz, T., Kuryliszyn, I., Liu, X., Sasaki, Y., and Furdyna, J. K., 2002, *Phys. Rev.* B, **65**, 201 303(R).